Eur. Phys. J. A **17**, 65–69 (2003)
DOI 10.1140/epja/i2002-10137-2

THE EUROPEAN PHYSICAL JOURNAL A

Spectroscopic information from different theoretical descriptions of (un)polarized (e, e′p) reactions

M. Radici[1], A. Meucci[1,a], and W.H. Dickhoff[2]

[1] Dipartimento di Fisica Nucleare e Teorica, Università di Pavia, and Istituto Nazionale di Fisica Nucleare, Sezione di Pavia, I-27100 Pavia, Italy
[2] Department of Physics, Washington University, St. Louis, MO 63130, USA

Received: 16 September 2002 / Revised version: 10 January 2003 /
Published online: 8 April 2003 –
Communicated by Th. Walcher

Abstract. We analyze the unpolarized and polarized electron-induced proton knockout reactions on ^{16}O in different kinematical settings using two theoretical approaches. The first one is based on a relativistic mean-field distorted-wave description of the bound and scattering states of the proton, including a fully relativistic electromagnetic current operator. The second approach adopts the same current operator, but describes the proton properties on the basis of microscopic calculations of the self-energy in ^{16}O below the Fermi energy and final-state damping in nuclear matter above the Fermi energy, using the same realistic short-range and tensor correlations. Good agreement with all unpolarized data is obtained at low and high Q^2 by using the same spectroscopic factors fixed by the low-Q^2 analysis. A reasonable agreement is achieved for polarization observables.

PACS. 25.30.Dh Inelastic electron scattering to specific states – 24.70.+s Polarization phenomena in reactions – 24.10.Jv Relativistic models – 24.10.Eq Coupled-channel and distorted-wave models

A long series of high-precision experiments on several nuclei [1–6] have generated a well-established tradition which singles out exclusive $(e, e'p)$ knockout reactions as the primary tool to explore the single-particle aspects of the nucleus. The experimental analysis has focused on the missing energy spectrum of the nuclear response, assigning specific quantum numbers and spectroscopic factors to the various peaks corresponding to orbitals close to the Fermi energy. In addition, the missing momentum dependence of these spectra has been studied, stimulating, for example, the exploration of the high-momentum components induced by nucleon-nucleon correlations inside nuclei [7,8]. The theoretical description of these reactions have usually been performed in the framework of the nonrelativistic distorted-wave impulse approximation (DWIA), including the Coulomb distortion of the electron and proton waves due to the presence of the nuclear field [1,9–11]. This approach was able to describe to a high degree of accuracy the shape of the experimental momentum distribution for several nuclei in a wide range of different kinematics [10,11]. However, a systematic rescaling of the normalization of the bound state, interpreted as the spectroscopic factor for the corresponding level, had to be applied in order to reproduce the magnitude of the experimental distribution [5,12]. This systematic deviation from the mean-field expectations has clearly identified the limits of this approximation. In fact, nowadays a clear picture has emerged in which a considerable mixing between single-hole states and more complicated configurations results in a fragmentation of the single-particle strength in several peaks around and beyond the Fermi surface. A further depletion of the single-particle strength is induced by short-range and tensor correlations between nucleon pairs in the ground state [13,14].

More recent $(e, e'p)$ experiments have been carried out at the Jefferson Laboratory (JLAB) [15,16] at higher momentum transfer Q^2. The analysis of this new kinematic domain required a substantial upgrade of several theoretical ingredients in order to incorporate all possible relativistic effects. Models based on relativistic DWIA (RDWIA) have been developed, where the Dirac equation is solved directly for the nucleon bound and scattering states [17–20] or, equivalently, a Schrödinger-like equation is solved and the spinor distortion by the Dirac scalar and vector potentials is incorporated in an effective current operator in the so-called effective Pauli reduction [20,21]. A successful description of the data has been achieved, but slightly different spectroscopic factors are deduced, because the relativistic optical potentials in general give a stronger residual final-state interaction (FSI)

[a] e-mail: andrea.meucci@pv.infn.it

than the corresponding nonrelativistic ones [19,22]. Moreover, the limits of validity of the older DWIA analysis *versus* RDWIA were not always properly explored, as discussed in ref. [23], resulting, for example, in a certain degree of ambiguity for the spectroscopic factors extracted at low energy.

Despite several sources of theoretical uncertainties (different equivalent potentials for FSI, relativistic effects on both FSI and spectroscopic factors, off-shell effects...), a microscopic treatment of the $(e, e'p)$ reaction mechanism at different kinematics is highly desirable. Results for a first attempt towards this goal were recently obtained in ref. [24] (see also ref. [25] concerning the treatment of FSI), where a successful analysis of low- and high-Q^2 data was performed using identical spectroscopic factors which were deduced at low Q^2. In the present paper, this analysis is extended to the data at high missing momentum of ref. [6] as well as to the JLAB experiment with polarization, as reported in ref. [16]. The results will then be compared with those obtained in ref. [23], where a RDWIA approach to low- and high-energy data was presented and a careful analysis of the limits of the nonrelativistic DWIA was carried out. The sensitivity to different off-shell prescriptions for the electromagnetic current operator will be also discussed [26], but the difference between spectroscopic factors obtained by nonrelativistic and relativistic analyses remains unsolved and its discussion is beyond the scope of this paper.

The basic ingredient of the calculation is the transition amplitude (omitting spin degrees of freedom for simplicity) [10,24],

$$J^{\mu}_{n}(\omega, \mathbf{q}, \mathbf{p}'_N, E_R) = \int \mathrm{d}\mathbf{p}\ \mathrm{d}\mathbf{p}'\ \chi^{(-)\,*}_{p'_N E_R n}(\mathbf{p}') \times \hat{J}^{\mu}_{\mathrm{eff}}(\mathbf{p}, \mathbf{p}', \mathbf{q}, \omega)\ \phi_{E_R n}(\mathbf{p})\ [Z_n(E_R)]^{\frac{1}{2}}\ , \quad (1)$$

where $\mathbf{q}$, ω are the momentum and energy transferred to the target ($Q^2 = q^2 - \omega^2$) and $\mathbf{p}'_N$ is the knocked-out nucleon momentum, leaving the residual nucleus in a well-defined state with energy E_R and quantum numbers n. The function $\phi_{E_R n}$ describes the overlap between the exact A-body initial state and the residual $(A-1)$-body state induced by producing a hole; $\chi^{(-)}_{p'_N E_R n}$ describes the same kind of overlap when producing the hole in the exact A-body final state [10]. The norm of $\phi_{E_R n}$ is 1 and $Z_n(E_R)$ is the spectroscopic factor associated with the removal process, *i.e.*, it corresponds to the probability that the residual nucleus can indeed be considered as the target nucleus with a hole. The boundary conditions of the eigenvalue problem for $\chi^{(-)}_{p'_N E_R n}$ are those of an incoming wave.

In the RDWIA of refs. [23,26], $\phi_{E_R n}$ is replaced by the solution of a Dirac equation [27] deduced in the context of a relativistic mean-field theory that satisfactorily reproduces global and single-particle properties of several nuclei [28]. For the scattering states the effective Pauli reduction is applied. The Darwin nonlocality factor, that contains the effect of the negative-energy components of the spinor, is reabsorbed in the current operator, which becomes an effective relativistic one-body operator depending on the Dirac scalar and vector potentials [20,21], as well as on the chosen off-shell prescription (cc1, cc2, or cc3) [26,29]. The function $\chi^{(-)}_{p'_N E_R n} \sim \chi^{(-)}_{p'_N}$ becomes a two-component spinor which solves the Schrödinger equation with the equivalent central and spin-orbit potentials expressed in terms of the original Dirac scalar and vector ones [30].

In ref. [24] the transition amplitude is evaluated by systematically applying the effective Pauli reduction to both the initial and final Dirac spinors, determining the relevant integrals in momentum space thus avoiding any effective momentum approximation (EMA) [21]. The current operator displays the same features as in the RDWIA discussed above, *i.e.*, it is an effective one-body relativistic operator depending on the Dirac scalar and vector potentials. In ref. [24] only the cc1 off-shell prescription has been considered for compatibility with older low-energy data analyses [31]. The scattering state of the (very energetic) proton is described in the eikonal approximation by a uniformly damped plane wave, or, equivalently, by a plane wave with a complex momentum $\mathbf{p}'_f = \mathbf{p}'_N + i\mathbf{p}_I$ [32,33]. The imaginary part p_I is microscopically justified by linking the proton absorption to the same process taking place in nuclear matter and by calculating the nucleon self-energy in a self-consistent manner with realistic short-range and tensor correlations [24,34]. The observed damping is also in agreement with expectations in different kinematic domains [35]; however, embedding the proton in nuclear matter prevents the inclusion of spin-orbit effects; therefore, the corresponding Darwin nonlocality factor for the final state is just 1. The function $\phi_{E_R n}$ is obtained from p-shell quasihole states deduced from the nucleon self-energy calculated for ^{16}O using realistic short-range and tensor correlations [8].

The hadronic tensor of the reaction, $W^{\mu\nu}$, involves an average over initial states and a sum over the undetected final states of bilinear products of the scattering amplitude (1). The differential cross-section for the $(\vec{e}, e'\vec{p})$ reaction, with initial beam helicity h and proton polarization component $\hat{s}$, becomes [10]

$$\begin{aligned}\frac{\mathrm{d}\sigma_{h\hat{s}}}{\mathrm{d}\mathbf{p}'_e \mathrm{d}\mathbf{p}'_N} &= \frac{e^4}{16\pi^2}\frac{1}{Q^4 p_e p'_e}\ L_{\mu\nu} W^{\mu\nu} \\ &\equiv \frac{e^4}{16\pi^2}\frac{1}{Q^4 p_e p'_e}\ L_{\mu\nu} \overline{\sum_i} \sum\!\!\!\!\!\!\int_f\ J^{\mu}_{n} J^{\nu\,*}_{n}\ \delta\left(E_f - E_i - \omega\right) \\ &= \frac{\mathrm{d}\sigma^0}{\mathrm{d}\mathbf{p}'_e \mathrm{d}\mathbf{p}'_N}\ \frac{1}{2}\ \left[1 + \mathbf{P}\cdot\hat{s} + h\,(A + \mathbf{P}'\cdot\hat{s})\right]\ ,\end{aligned} \quad (2)$$

where p_e, p'_e are the initial and final electron momenta and $L_{\mu\nu}$ is the lepton tensor. The coefficients of the linear expansion are the induced polarization $\mathbf{P}$, the electron analyzing power A, and the polarization transfer coefficient $\mathbf{P}'$. The reference frame in the polarimeter is formed by the direction of $\mathbf{p}'_N$ (L-component), the direction of $\mathbf{q}\times\mathbf{p}'_N$ (N-component) and $\hat{N}\times\hat{L}$ (T-component). In coplanar kinematics, as is the case for the E89033 experiment at JLAB [16], only P^N, P'^L and P'^T survive. When summing

over the recoil proton polarization and the beam helicity, the usual unpolarized cross-section $\mathrm{d}\sigma^0$ is recovered.

In fig. 1 we first reconsider the unpolarized $^{16}\mathrm{O}(e, e'p)$ reaction leading to the ground state and the first excited state of $^{15}\mathrm{N}$ with $p\frac{1}{2}$ and $p\frac{3}{2}$ quantum numbers, respectively. In the upper panel, data have been collected in parallel kinematics ($\mathbf{p}'_N \parallel \mathbf{q}$) at a constant proton energy of 90 MeV in the center-of-mass system [36]. They are presented in the form of the reduced cross-section

$$n(\mathbf{p}_m, E_m) \equiv \frac{\mathrm{d}\sigma^0}{\mathrm{d}\mathbf{p}'_e \mathrm{d}\mathbf{p}'_N} \frac{1}{K\sigma_{ep}} , \qquad (3)$$

as a function of the missing momentum $\mathbf{p}_m = \mathbf{p}'_N - \mathbf{q}$ at the considered missing energy E_m, where K is a suitable kinematic factor and σ_{ep} is the elementary (half–off-shell) electron-proton cross-section [29]. For ease of viewing, the results for the transition to the $p\frac{1}{2}$ ground state have been multiplied by 40. The solid lines refer to the calculations employing the p-shell quasihole states for $^{16}\mathrm{O}$ in a nonrelativistic framework, as discussed in ref. [31]. The spectroscopic factors extracted from the data are $Z_{p1/2} = 0.644$ and $Z_{p3/2} = 0.537$, respectively. The dashed lines show the results of the RDWIA analysis with the same cc1 off-shell prescription; dot-dashed and dotted lines indicate the results when using the cc2 and cc3 recipes, respectively. Hence, the comparison among dashed, dot-dashed, and dotted lines shows the evolution in p_m of the theoretical uncertainty related to off-shellness at this kinematics. Relativistic mean-field bound states are obtained by solving Hartree-Bogoliubov equations with finite-range interactions [27]. The proton scattering wave is deduced from relativistically equivalent energy-dependent optical potentials [30]. The resulting spectroscopic factors, $Z_{p1/2} = 0.708$ and $Z_{p3/2} = 0.602$, have been obtained by a χ^2 fit using the cc3 current, which gives an overall better description of the $(e, e'p)$ observables, particularly for the left-right asymmetry.

In the middle panel, the analysis of the same reaction is extended to higher missing momenta. The experiment was performed at the MAMI accelerator in Mainz [6] by mixing six different kinematics, with a central value of 196 MeV for the outgoing proton energy. The different data sets are displayed with alternating markers. Again the solid lines refer to the calculation employing the p-shell quasihole states but with an effective relativistic current operator and an eikonal microscopic description of FSI as discussed above (see ref. [24] for further details). The dashed, dot-dashed, and dotted lines still refer to the RDWIA analysis with the cc1, cc2, and cc3 off-shell prescriptions for the electromagnetic current, respectively. The same rescaling spectroscopic factors are adopted for the theoretical curves as in the upper panel. The $p\frac{1}{2}$ results are conveniently multiplied by a factor 500. The overall agreement is still rather satisfactory, even if the calculation based on the quasihole state gives on average a worse performance than the RDWIA ones (among which the cc3 recipe gives the best description of data). This is probably due to the lack of a full treatment of FSI effects inside the eikonal approximation, particularly those related to spin-orbit contributions

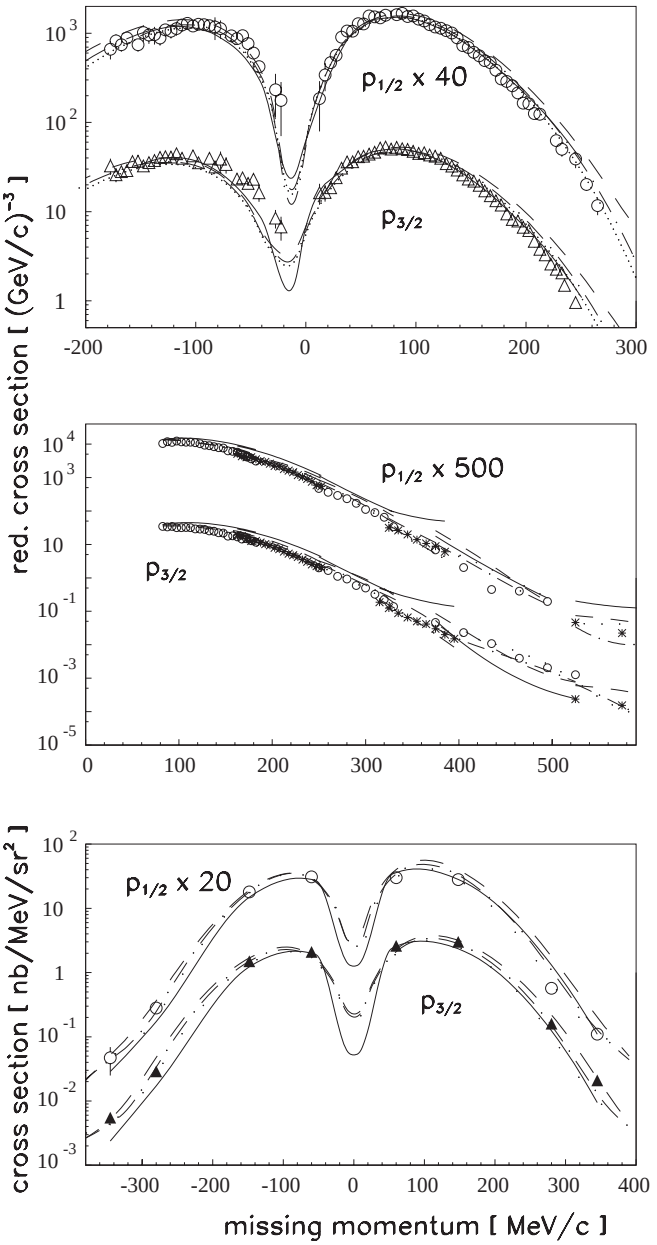

Fig. 1. Upper panel: reduced cross-section for the $^{16}\mathrm{O}(e, e'p)^{15}\mathrm{N}$ transition to the ground state $p\frac{1}{2}$ and first excited state $p\frac{3}{2}$ of $^{15}\mathrm{N}$ at $E_p = 90$ MeV constant proton energy in the center-of-mass system in parallel kinematics [36]. Middle panel: reduced cross-section for the same reaction at six different kinematics [6], indicated by alternating markers. Lower panel: cross-section for the same reaction but at $Q^2 = 0.8$ (GeV/c)^2 in perpendicular kinematics [15]. Data for the $p\frac{1}{2}$ state have been multiplied by 40, 500 and 20, respectively. Solid lines show the results when using the quasihole spectral function for the bound state (see text) with spectroscopic factors $Z_{p1/2} = 0.644$ and $Z_{p3/2} = 0.537$ in all panels [24,31]. Dashed, dot-dashed, and dotted lines represent the results of the RDWIA approach with cc1, cc2, cc3 off-shell prescriptions, respectively (see text). All the RDWIA curves in all panels have been rescaled by the spectroscopic factors $Z_{p1/2} = 0.708$ and $Z_{p3/2} = 0.602$, obtained by a χ^2 fit to the data of ref. [36] using the cc3 current.

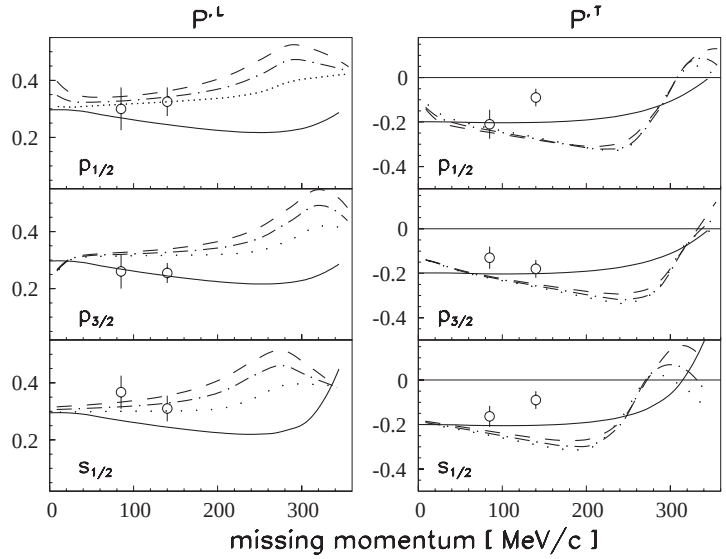

Fig. 2. Polarization transfer components P'^L, P'^T for the ^{16}O$(\vec{e}, e'\vec{p})$ reaction at $Q^2 = 0.8$ (GeV/c)^2 in perpendicular kinematics [16] leading to the ^{15}N $p\frac{1}{2}$, $p\frac{3}{2}$ and $s\frac{1}{2}$ residual states. Solid, dashed, dot-dashed, and dotted lines as in fig. 1.

which are, on the contrary, conveniently parametrized in the RDWIA optical potential. At very high missing momenta the agreement is somewhat less satisfactory, but in this domain the contribution to the single-particle strength is only an extremely tiny fraction of the 10% of the protons that are expected to be associated with high momenta due to short-range correlations [7,8].

In the lower panel, the same reaction is considered at constant $(\mathbf{q}, \omega)$ with $Q^2 = 0.8$ (GeV/c)^2 [15]. The data now refer to the differential unpolarized cross-section dσ^0, avoiding any model dependence in the experimental analysis contained in the off-shell behavior of σ_{ep} [29]. The $p\frac{1}{2}$ results are multiplied by a factor 20. The theoretical curves have the same meaning as in the middle panel and are rescaled again by the same spectroscopic factors. The agreement with the data is very good also in this case. This outcome is particularly welcome, since the spectroscopic factors correspond to a nuclear property that must be independent of the probe scale Q^2. Obviously, different models give different spectroscopic factors, but it is important to note that we do not observe any energy scale dependence of these factors over a wide kinematical range. The approximation introduced in the eikonal treatment of FSI, specifically the absence of any spin-orbit effect, does not severely affect the agreement between the solid lines and the data. Similarly, the sensitivity to the off-shell ambiguity in the electromagnetic current operator is relatively weak. After all, it is well known that the cross-section is not particularly sensitive to these uncertainties within a range of about 10%. In ref. [24] more sensitive observables than the unpolarized cross-section were considered. Good agreement with these data was maintained but, at the same time, the limitations of this approximation emerged, particularly in the left-right asymmetry. Here, for the same kinematic conditions we extend the analysis to polarization observables in order to further test the capabilities of the models.

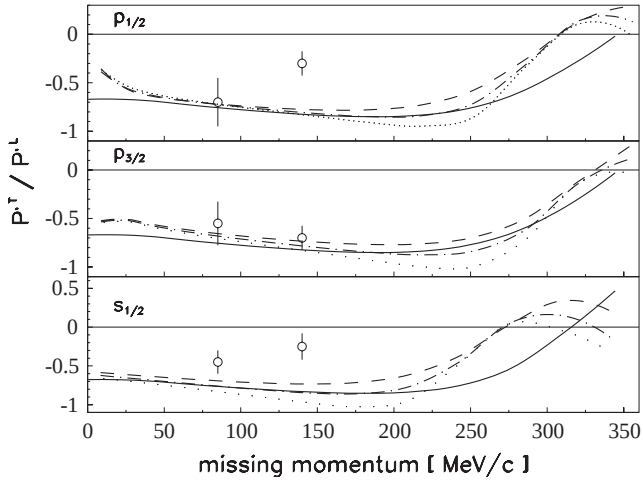

Fig. 3. The ratio P'^T/P'^L for the ^{16}O$(\vec{e}, e'\vec{p})$ reaction at $Q^2 = 0.8$ (GeV/c)^2 in perpendicular kinematics [16] leading to the ^{15}N $p\frac{1}{2}$, $p\frac{3}{2}$ and $s\frac{1}{2}$ residual states. Notations as in fig. 1.

In figs. 2 and 3 the polarization transfer components P'^L, P'^T and their ratio P'^T/P'^L are shown as functions of the missing momentum p_m, respectively, for the ^{16}O$(\vec{e}, e'\vec{p})$ reaction at $Q^2 = 0.8$ (GeV/c)^2 and constant $(\mathbf{q}, \omega)$ for the transitions to the ^{15}N ground state $p\frac{1}{2}$, the first $p\frac{3}{2}$ state at $E_m = 6.32$ MeV and the weak peak with quantum numbers $s\frac{1}{2}$ rising above a continuum background at $E_m \sim 28$ MeV [16]. Solid, dashed, dot-dashed, and dotted lines refer to the same calculations as in fig. 1. For these observables and at this kinematics, the sensitivity to off-shell effects is at most $\lesssim 15\%$. The overall agreement with the data is still good, particularly for the microscopic calculations with the $p\frac{3}{2}$ quasihole state that performs even better than the RDWIA analysis presented here or obtained by other groups [16]. This

fact is remarkable, since the RDWIA analysis depends on mean-field phenomenological potentials with several parameters fitted to the considered target and energy domain, while the calculation with quasihole states is basically parameter free. In fact, from eq. (2) it is easy to verify that the polarization observables are given by ratios between a specific spin projection of the cross-section and the unpolarized cross-section, eliminating any sensitivity to the spectroscopic factor which is anyway fixed from the very beginning to the low-energy data of ref. [36]. Moreover, the calculations of the solid lines include an attempt of a microscopic description of FSI in the framework of the eikonal approximation in a way which is consistent with the description of the bound state. The limitations of such an approach are more evident in the $j = \frac{1}{2}$ case, where, contrary to the RDWIA analysis, the absence of any spin-orbit effects is most likely responsible for the worse agreement. In any case, the second P'^T data point for both $p\frac{1}{2}$ and $s\frac{1}{2}$ shells appears not reproducible in both calculations, causing the theoretical ratio P'^T/P'^L to deviate substantially from the experiment. A further analysis of this unexplained feature is needed, but it is beyond the scope of this paper.

In summary, we have analyzed the unpolarized and polarized proton knockout reactions on ^{16}O at different kinematics with two theoretical approaches. The RDWIA is based on a relativistic mean-field description of the proton bound state and on the effective Pauli reduction of the final Dirac spinor, leading to a Schrödinger-equivalent mean-field description of residual FSI and to an effective relativistic electromagnetic current operator which depends on the Dirac scalar and vector potentials. The same kind of Pauli reduction (and resulting current operator) is used for both initial and final states in the second approach, where a microscopic description of the bound-state properties is obtained by solving the Dyson equation with a nucleon self-energy which includes realistic short-range and tensor correlations for ^{16}O. As an attempt towards a more complete microscopic treatment, the proton scattering wave is then generated in the eikonal approximation by microscopically calculating the damping of a plane wave as a solution of the Dyson equation for the nucleon self-energy including the same realistic short-range and tensor correlations between the struck proton and the surrounding nucleons in nuclear matter. Good agreement with data is observed for unpolarized reactions at low and high Q^2 by using the same spectroscopic factors fixed by the low-Q^2 analysis, thus indicating that no Q^2-dependence of these factors is observed. Moreover, a reasonable agreement with polarization observables is achieved, even though a more detailed analysis is required to understand the observed discrepancies.

This work is supported by the U.S. National Science Foundation under Grant No. PHY-9900713. We acknowledge fruitful discussions with C. Giusti and F.D. Pacati.

References

1. S. Frullani, J. Mougey, Adv. Nucl. Phys. **14**, 1 (1984).
2. J. Mougey *et al.*, Nucl. Phys. A **262**, 461 (1976).
3. M. Bernheim *et al.*, Nucl. Phys. A **375**, 381 (1982).
4. P.K.A. de Witt Huberts, J. Phys. G **16**, 507 (1990).
5. L. Lapikás, Nucl. Phys. A **553**, 297c (1993).
6. K.I. Blomqvist *et al.*, Phys. Lett. B **344**, 85 (1995).
7. H. Müther, W.H. Dickhoff, Phys. Rev. C **49**, R17 (1994).
8. H. Müther, A. Polls, W.H. Dickhoff, Phys. Rev. C **51**, 3040 (1995).
9. S. Boffi, C. Giusti, F.D. Pacati, Phys. Rep. **226**, 1 (1993).
10. S. Boffi, C. Giusti, F.D. Pacati, M. Radici, *Electromagnetic Response of Atomic Nuclei*, Oxford Studies in Nuclear Physics, Vol. **20** (Clarendon Press, Oxford, 1996).
11. J.J. Kelly, Adv. Nucl. Phys. **23**, 75 (1996).
12. V.R. Pandharipande, I. Sick, P.K.A. de Witt Huberts, Rev. Mod. Phys. **69**, 981 (1987).
13. W.H. Dickhoff, H. Müther, Rep. Prog. Phys. **55**, 1947 (1992).
14. W.H. Dickhoff, Phys. Rep. **242**, 119 (1994).
15. The Jefferson Lab Hall A Collaboration (J. Gao *et al.*), Phys. Rev. Lett. **84**, 3265 (2000).
16. The Jefferson Lab Hall A Collaboration (S. Malov *et al.*), Phys. Rev. C **62**, 057302 (2000).
17. A. Picklesimer, J.W. Van Orden, Phys. Rev. C **40**, 290 (1989).
18. Y. Jin, D.S. Onley, Phys. Rev. C **50**, 377 (1994).
19. J.M. Udías, J.A. Caballero, E. Moya de Guerra, J.R. Vignote, A. Escuderos, Phys. Rev. C **64**, 024614 (2001).
20. M. Hedayati-Poor, J.I. Johansson, H.S. Sherif, Phys. Rev. C **51**, 2044 (1995).
21. J.J. Kelly, Phys. Rev. C **60**, 044609 (1999).
22. S. Boffi, C. Giusti, F.D. Pacati, F. Cannata, Nuovo Cimento A **98**, 291 (1987).
23. A. Meucci, C. Giusti, F.D. Pacati, Phys. Rev. C **64**, 014604 (2001).
24. M. Radici, W.H. Dickhoff, E. Roth Stoddard, Phys. Rev. C **66**, 014613 (2002).
25. D. Debruyne, J. Ryckebusch, S. Janssen, T. Van Cauteren, Phys. Lett. B **527**, 62 (2002).
26. A. Meucci, Phys. Rev. C **65**, 044601 (2002).
27. W. Pöschl, D. Vretenar, P. Ring, Comput. Phys. Commun. **103**, 217 (1997).
28. G.A. Lalazissis, J. König, P. Ring, Phys. Rev. C **55**, 540 (1997).
29. T. de Forest jr., Nucl. Phys. A **392**, 232 (1983).
30. E.D. Cooper, S. Hama, B.C. Clark, R.L. Mercer, Phys. Rev. C **47**, 297 (1993).
31. A. Polls, M. Radici, S. Boffi, W.H. Dickhoff, H. Müther, Phys. Rev. C **55**, 810 (1997).
32. A. Bianconi, M. Radici, Phys. Rev. C **56**, 1002 (1997).
33. F. Cannata, J.P. Dedonder, L. Lesniak, Phys. Rev. C **33**, 1888 (1986).
34. W.H. Dickhoff, E.P. Roth, Acta Phys. Pol. B **33**, 65 (2002).
35. The NE18 Collaboration (N.C.R. Makins *et al.*), Phys. Rev. Lett. **72**, 1986 (1994).
36. M. Leuschner *et al.*, Phys. Rev. C **49**, 955 (1994).